

Characterizations of Ga-doped ZnO films on Si (111) prepared by atmospheric pressure metal-organic chemical vapor deposition

Yen-Chin Huang, Zhen-Yu Li, Li-Wei Weng, Wu-Yih Uen, Shan-Ming Lan, Sen-Mao Liao, Tai-Yuan Lin, Yu-Hsiang Huang, Jian-Wen Chen, Tsun-Neng Yang, and Chin-Chen Chiang

Citation: *Journal of Vacuum Science & Technology A* **27**, 1260 (2009); doi: 10.1116/1.3212895

View online: <http://dx.doi.org/10.1116/1.3212895>

View Table of Contents: <http://scitation.aip.org/content/avs/journal/jvsta/27/6?ver=pdfcov>

Published by the AVS: Science & Technology of Materials, Interfaces, and Processing

Articles you may be interested in

[n -type, p -type and semi-insulating ZnO:N thin film growth by metal organic chemical vapor deposition with N H 3 doping](#)

J. Vac. Sci. Technol. B **27**, 1904 (2009); 10.1116/1.3151829

[Effect of growth temperature on the characteristics of ZnO films grown on Si\(111\) substrates by metal-organic chemical vapor deposition](#)

J. Vac. Sci. Technol. A **26**, 224 (2008); 10.1116/1.2835090

[Evolution of the electrical and structural properties during the growth of Al doped ZnO films by remote plasma-enhanced metalorganic chemical vapor deposition](#)

J. Appl. Phys. **102**, 043709 (2007); 10.1063/1.2772569

[Raman and photoluminescence of ZnO films deposited on Si \(111\) using low-pressure metalorganic chemical vapor deposition](#)

J. Vac. Sci. Technol. A **21**, 979 (2003); 10.1116/1.1580836

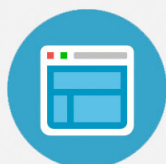
[Transparent and conductive Ga-doped ZnO films grown by low pressure metal organic chemical vapor deposition](#)

J. Vac. Sci. Technol. A **15**, 1063 (1997); 10.1116/1.580430



Re-register for Table of Content Alerts

Create a profile.



Sign up today!



Characterizations of Ga-doped ZnO films on Si (111) prepared by atmospheric pressure metal-organic chemical vapor deposition

Yen-Chin Huang

Department of Electronic Engineering, College of Electrical Engineering and Computer Science, Chung Yuan Christian University, Chung-Li 32023, Taiwan

Zhen-Yu Li

Department of Photonics and Institute of Electro-Optical Engineering, National Chiao Tung University, 1001 TA Hsueh Road, Hsinchu 30010, Taiwan

Li-Wei Weng, Wu-Yih Uen,^{a)} Shan-Ming Lan, and Sen-Mao Liao

Department of Electronic Engineering, College of Electrical Engineering and Computer Science, Chung Yuan Christian University, Chung-Li 32023, Taiwan

Tai-Yuan Lin

Institute of Optoelectronic Sciences, National Taiwan Ocean University, Keelung 222, Taiwan

Yu-Hsiang Huang, Jian-Wen Chen, Tsun-Neng Yang, and Chin-Chen Chiang^{b)}

Institute of Nuclear Energy Research, P.O. Box 3-11, Lungtan 32500, Taiwan

(Received 7 July 2009; accepted 3 August 2009; published 14 September 2009)

Gallium-doped ZnO films were grown on *p*-Si(111) substrates by atmospheric pressure metal-organic chemical vapor deposition (AP-MOCVD) using diethylzinc and water as reactant gases and triethyl gallium (TEG) as a *n*-type dopant gas. The structural, electrical, and optical properties of ZnO:Ga films obtained by varying the flow rate of TEG from 0.56 to 3.35 $\mu\text{mol}/\text{min}$ were examined. X-ray diffraction patterns and scanning electron microscopy images indicated that Ga doping plays a role in forming microstructures in ZnO films. A flat surface with a predominant orientation (101) was obtained for the ZnO:Ga film fabricated at a flow rate of TEG = 2.79 $\mu\text{mol}/\text{min}$. This film also revealed a lowest resistivity of $4.54 \times 10^{-4} \Omega \text{ cm}$, as measured using the van der Pauw method. Moreover, low temperature photoluminescence (PL) emission recorded at 12 K demonstrated the Burstein Moss shift of PL line from 3.365 to 3.403 eV and a line broadening from 100 to 165 meV as the TEG flow rate varied from 0.56 to 2.79 $\mu\text{mol}/\text{min}$. This blueshift behavior of PL spectra from ZnO:Ga films features the degeneracy of semiconductor, which helps to recognize the enhancing of transparency and conductivity of ZnO films fabricated by AP-MOCVD using Ga-doping technique. © 2009 American Vacuum Society.

[DOI: 10.1116/1.3212895]

I. INTRODUCTION

Zinc oxide (ZnO) is a wide band gap semiconductor with a direct band gap of 3.37 eV at room temperature. It demonstrates high thermal and chemical stability, good electrical conductivity, and high optical transparency. In addition, it has a large exciton bind energy of 60 meV, which is 2.4 times larger than that of GaN. ZnO is extensively studied because of its potential applications in widespread fields, such as a transparent conductive layer and/or an antireflection coating for amorphous-silicon (*a*-Si) and Cu(InGa)Se₂-based solar cells.¹⁻³ Moreover, ultraviolet light emitting devices⁴ and laser diodes⁵ based on this material are also possible. Undoped ZnO films usually show *n*-type conductivity but with a high resistivity due to the intrinsic defects of oxygen vacancies and zinc interstitials.⁶ Therefore, high conductive films can be obtained only by doping metal elements that substitute zinc sites.^{7,8} Compared to undoped

ZnO, the doped one has a lower resistivity and better stability of electrical properties. It is well known that group III elements such as Al,⁹ In,¹⁰ Ga,¹¹ and B (Ref. 12) act as donors in ZnO. Among these metal dopants, Ga seems to be a promising one because the covalent bond length of Ga–O (0.192 nm) is slightly smaller than that of Zn–O (0.197 nm) and only small ZnO lattice deformations are caused even high concentrations of Ga are introduced.

For the deposition of Ga-doped ZnO (ZnO:Ga) films, a number of growth techniques such as, magnetron sputtering,¹³⁻¹⁵ pulsed laser deposition,^{16,17} molecular beam epitaxy,¹⁸ atmospheric pressure metal-organic chemical vapor deposition (AP-MOCVD),¹⁹ plasma enhanced metal-organic chemical vapor deposition,²⁰ and low-pressure metal-organic chemical vapor deposition^{21,22} were used.

In our study, we fabricate ZnO:Ga films by AP-MOCVD. Little has been known about the growth of ZnO:Ga film by this method. As is known, AP-MOCVD is a simple fabrication process and cost competitive for device applications of thin films. It is capable of producing high growth rates over large areas. Doped films can be deposited by introducing the

^{a)} Author to whom correspondence should be addressed; electronic mail uenwuyih@ms37.hinet.net

^{b)} Electronic mail: chin099983@hotmail.com

TABLE I. Summary of the progress in ZnO:Ga films produced by MOCVD.

Ref.	Method	Substrate	Carrier concentration (cm ⁻³)	Mobility (cm ² /V s)	Resistivity (Ω cm)	Transmittance (%)
21	LP-MOCVD	Sapphire	2.47×10^{19}	>90
23	AP-MOCVD	Glass	6.96×10^{20}	30.4	3.6×10^{-4}	~85
11	LP-MOCVD	Glass	4×10^{21}	6.01	2.6×10^{-4}	>85
24	AP-MOCVD	Glass	3.47×10^{20}	60	3×10^{-4}	~85
25	LP-MOCVD	ZnO	1.65×10^{21}	27.4	2.21×10^{-4}	>90

dopant into the gas phase, and the extent of doping can be easily controlled by the concentration of dopant in gas phase. We have recently reported the characterizations of absorption and transmission spectra of ZnO:Ga films fabricated on glass substrates by AP-MOCVD.²³ ZnO:Ga films with a low resistivity of 3.6×10^{-4} Ω cm and a high transparency of 85% were achieved, which are expectable for being used as transparent electrodes in optoelectronic device applications. For a reference, Table I summarizes some recent progress concerning the quality of ZnO:Ga films produced by MOCVD. In the present work, we report the characterizations of ZnO:Ga films fabricated on Si(111) substrate. The structural, electrical, and optical properties of ZnO:Ga films doped to different degrees were systematically examined to recognize the doping capability of Ga elements in ZnO film and also the availability of ZnO:Ga for a transparent conductive film.

II. EXPERIMENTS

ZnO thin films were deposited using a custom-made one-flow AP-MOCVD system. The substrates are 2 in. (111)-oriented, *p*-type Si wafers with a resistivity of 1–3 kΩ cm. The growth chamber is a water-cooled vertical reactor. The substrate susceptor is made of graphite, 2 in. in diameter and coated with a SiC film on top surface by CVD technique. Diethylzinc (DEZn) and water were used as the sources of Zn and O, respectively. Besides, triethyl gallium (TEG) was used as the doping gas for Ga. N₂ was used as the carrier gas for the growth of ZnO:Ga films. Before the ZnO:Ga film growth, an undoped ZnO buffer layer of about 5–10 nm was grown at a low temperature of 200 °C and with a gas flow ratio of [H₂O]: [DEZn] (VI/II ratio)=6.84. Then, the growths of ZnO:Ga top layers were conducted at 400 °C with their VI/II ratios being kept at 1.37 and growth time duration set for 30 min to achieve a thickness of about 200–300 nm. Specimens for comparison were fabricated with different TEG flow rates ranging from 0.56 to 3.35 μmol/min for Ga doping.

The crystalline structure of the ZnO:Ga thin films was analyzed by powder x-ray diffraction (XRD) (Bruker AXS Diffraktometer D8) using Cu Kα line as the x-ray source ($\lambda=1.54056$ Å). The surface morphology and thickness of ZnO films were examined by a scanning electron microscope (SEM) (JEOL-6700F) at an accelerating voltage of 10 kV. The resistivity, carrier concentration, and mobility of films were measured at room temperature by Hall measurements

using the van der Pauw method. The optical properties were characterized by photoluminescence (PL) measurements performed at 12 K. PL spectra were excited with the 325 nm line of a He–Cd laser.

III. RESULTS AND DISCUSSION

Figure 1 shows the XRD patterns of ZnO:Ga film deposited on *p*-Si(111) substrate under the TEG flow rate of 0.56–3.35 μmol/min. As can be seen from Fig. 1, all the films exhibit grain structures with a preferential orientation of (101) accompanied by a weak (002) peak. This result is quite different from those conventionally investigated, such as that reported in Ref. 26 where heavily Ga-doped films were examined. The (101) peak retains its intensity while the (002) peak gets weaker decreases with increasing the TEG flow rate to 2.79 μmol/min and somehow regains its intensity again with a further increase in TEG flow rate to

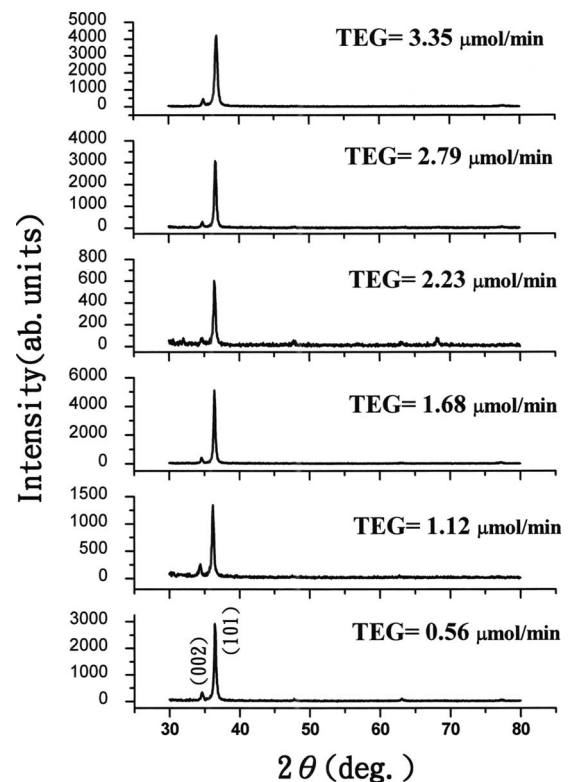


FIG. 1. XRD patterns of ZnO:Ga films fabricated with different TEG flow rates.

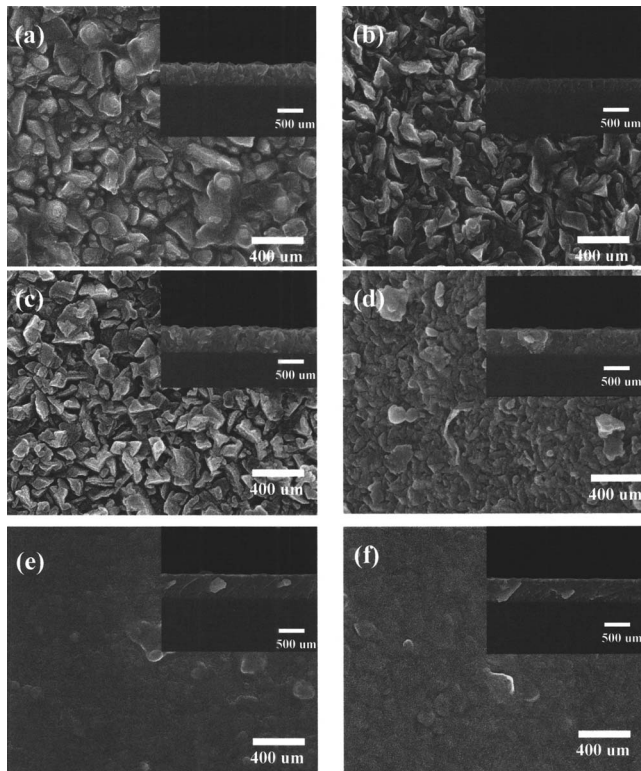


FIG. 2. SEM top-view images of ZnO:Ga films deposited with different TEG flow rates: (a) 0.56, (b) 1.12, (c) 1.68, (d) 2.23, (e) 2.79, and (f) 3.35 $\mu\text{mol}/\text{min}$. The inset of each figure shows the corresponding cross-sectional image.

3.35 $\mu\text{mol}/\text{min}$. The results described above imply that the Ga elements involved in ZnO film would influence the grain formation therein. Although it is suggested in Ref. 26 that the Ga doping causes the grains to grow without any predominant direction, in the present study the Ga doping was found to dominate the film growth with the appearance of $\{10\bar{1}1\}$ planes on top. Different results presented above are probably due to the different methods used for growing ZnO:Ga, however, further studies must be conducted to clarify the details.

The SEM surface images of ZnO:Ga thin films fabricated with various TEG flow rates are shown in Figs. 2(a)–2(e). Also, the cross-sectional images of these films are shown in the respective inset of these figures. It is obvious that ZnO:Ga films fabricated with the TEG flow rates ranging from 0.56 to 1.68 $\mu\text{mol}/\text{min}$ exhibit surface morphologies full of irregular grain structures. Those grains can be roughly categorized into the larger ones and the smaller ones according to their sizes, which have made the whole film surfaces become very rugged. However, a more homogeneous formation of grains is observable when the TEG flow rate is increased to 2.23 $\mu\text{mol}/\text{min}$ as demonstrated in Fig. 2(d) and the corresponding inset. In particular, as exhibited in Figs. 2(e) and 2(f), the ZnO:Ga films fabricated with a TEG flow rate over 2.79 $\mu\text{mol}/\text{min}$ show relatively uniform grain structures and their cross-sectional SEM images manifest the top surface of these films to be very flat compared to those grown with the TEG flow rates lower than 2.23 $\mu\text{mol}/\text{min}$.

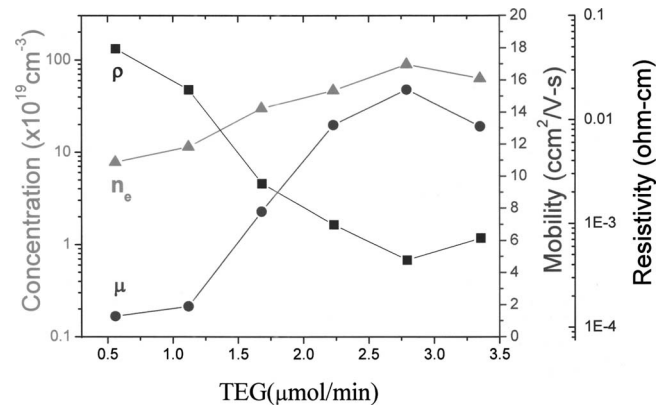


FIG. 3. Resistivity, electron concentration, and mobility of ZnO:Ga films deposited with various TEG flow rates.

Analogous results have been found on heavily Ga-doped films evaluated by atomic force microscopy and explained by modeling the grain formation considering the Ga-doping effect.²⁷ It is noticeable that the film surface changes from an irregular structure to homogeneous morphologies with an increase in TEG flow rate to over 2.23 $\mu\text{mol}/\text{min}$ and therefore the grain boundaries are also believed to be simultaneously reduced.

Figure 3 displays the resistivity (ρ), electron concentration (n_e), and Hall mobility (μ_H) of ZnO:Ga films as a function of the TEG flow rate. The undoped ZnO shows p -type conductivity, with ρ , μ_H , and hole concentration measured as 0.7516 $\Omega\text{ cm}$, 42.1 $\text{cm}^2\text{ V}^{-1}\text{ s}^{-1}$, and $1.97 \times 10^{17}\text{ cm}^{-3}$, respectively. As known, the intrinsic conductivity of ZnO is greatly influenced by the point defects produced therein. The p -type conductivity of undoped ZnO has been reported to be possibly due to the formation of Zn vacancies.²⁸ On the other hand, Ga is a n -type dopant that replaces zinc atoms (Ga_{Zn}) or forms interstitial atom (Ga_i) in ZnO, which increases the free electron concentration in the films. It can be seen that the resistivity of ZnO:Ga thin film decreases initially with increasing TEG flow rate and achieves a minimum value of $4.54 \times 10^{-4}\text{ }\Omega\text{ cm}$ at the TEG flow rate = 2.79 $\mu\text{mol}/\text{min}$. Then it increases conversely with a further increase in TEG flow rate. Whereas, the electron concentration increases gradually with increasing TEG flow rates from 0.56 to 2.79 $\mu\text{mol}/\text{min}$ and reaches a maximum value of $8.93 \times 10^{20}\text{ cm}^{-3}$. However, a further increase in TEG flow rate to 3.35 $\mu\text{mol}/\text{min}$ makes the electron concentration reduce to $6.28 \times 10^{20}\text{ cm}^{-3}$. Obviously, the Ga atoms in the films have a tendency to occupy interstitial sites as neutral defect, and even substitute oxygen site as an acceptor at higher doping concentrations, which is responsible for the decrease in electron concentration when the TEG flow rate is increased to 3.35 $\mu\text{mol}/\text{min}$. This carrier compensation phenomenon was also observed by Hu *et al.*¹⁹ for ZnO:Ga layers at high doping level. Moreover, the Hall mobility initially increases with the TEG flow rate and begins to decrease after a maximum value of $15.4\text{ cm}^2\text{ V}^{-1}\text{ s}^{-1}$ is achieved at the TEG flow rate = 2.79 $\mu\text{mol}/\text{min}$. As is reported, the Hall mobility (μ_H) can be expressed as²⁹

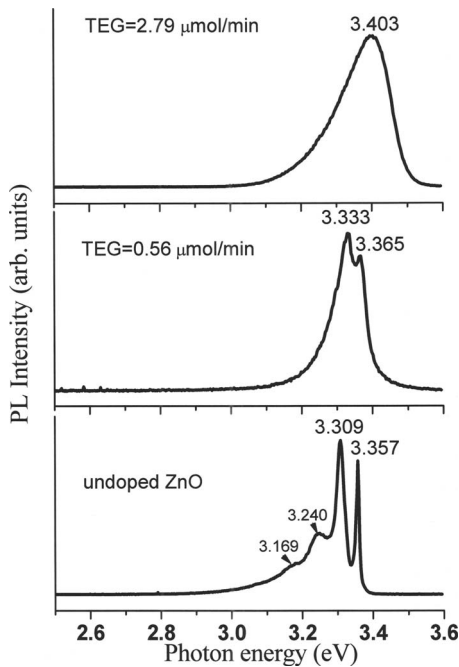


Fig. 4. PL spectra of undoped and Ga-doped ZnO films measured at 12 K.

$$\frac{1}{\mu_H} = \frac{1}{\mu_i} + \frac{1}{\mu_g},$$

where μ_i and μ_g are the mobilities dominated by impurity scattering and grain boundary scattering, respectively. μ_i should decrease with increasing TEG flow rate since the amount of Ga atoms incorporated in ZnO film is increased. Hence, it is reasonable to consider that the increase in μ_H with increasing TEG flow is mainly dominated by μ_g . As demonstrated in both XRD and SEM results described above, the grain structure is simplified and exhibits a relatively flat surface as the TEG flow rate is increased to over 2.79 $\mu\text{mol}/\text{min}$. This should be connected to a reduction in the area of grain boundaries, which should have been beneficial for elevating μ_g and therefore μ_H . That is to say, the increase in Hall mobility is due to the reduction in scattering from the grain boundaries. However, a further raise of TEG flow rate to 3.35 $\mu\text{mol}/\text{min}$ might enhance the Ga-related donor impurity, acceptor impurity, and/or defect scatterings to reduce μ_i , which would result in lowering μ_H , too.

Figure 4 shows PL spectra of undoped and Ga-doped ZnO films measured at 12 K. As can be seen, the PL spectrum of undoped ZnO displays several emission lines near ZnO band edge, such as 3.357, 3.309, 3.240, and 3.169 eV. The emission line at 3.357 eV is attributed to the recombination of excitons bound to neutral acceptors³⁰ or those bound to neutral donors.³¹ The strongest emission line at 3.309 eV is assigned to the donor-acceptor pair recombinations, accompanied by two LO-phonon replicas at 3.240 eV (1-LO) and 3.169 eV (2-LO).³² In contrast, the PL spectrum of Ga-doped ZnO film fabricated with a TEG flow rate of 0.56 $\mu\text{mol}/\text{min}$ is dominated by the emissions at 3.365 and 3.333 eV, which are related to the excitons bound to neutral donors.³³

Finally, for the film fabricated with a TEG flow rate of 2.79 $\mu\text{mol}/\text{min}$, the excitonic emission seems to be embedded in a wide band-to-band transition with a blueshift of the emission peak to 3.403 eV. No visible emissions are discovered for all PL spectra. This implies that the doping of Ga elements into the ZnO lattice does not bring about the defects responsible for deep level related emissions.²¹ The origins of the blueshift and linewidth broadening for the PL emission of heavily doped films are further analyzed below. Figure 5 shows (a) the normalized PL spectra measured at 12 K and (b) the peak position and full width at half maximum (FWHM) of ZnO:Ga films fabricated with various TEG flow rates ranging from 0.56 to 3.35 $\mu\text{mol}/\text{min}$. As the TEG flow rate increases from 0.56 to 2.79 $\mu\text{mol}/\text{min}$, the PL peak also shifts from 3.365 to 3.403 eV and meanwhile the FWHM of PL spectrum also increases from 100 to 165 meV. Two plausible mechanisms are considered to be responsible for the blueshift and linewidth broadening of PL spectra related to the well-known Burstein–Moss effect.^{34,35} The origin of this effect is the shift of the Fermi level (E_F) to above the bottom of the conduction band (E_c) as the doping degree surpasses the degeneracy limit. Thus, the peak position of PL spectra shifts to higher energies following Fermi level, as described by the equation below,³⁶

$$E_F - E_c = \frac{\hbar^2}{2m_e^*} (3\pi^2 n)^{2/3}, \quad (1)$$

where n represents the net electron concentration, \hbar the reduced Planck constant, and m_e^* the effective electron mass. Furthermore, due to indirect transitions (violating the k selection rule) between the filled states in the conduction band and valence band, the FWHM of PL was found empirically to increase with the energy shift.³⁷ The indirect character of such transitions was ascribed to the scattering of carriers by ionized donors and Auger processes.³⁸ Otherwise, some previous reports indicated a clear redshift due to the band tailing effect for their PL spectra of ZnO:Ga films.^{8,18,21} Such a variation in PL spectra is interpreted as mainly due to a band gap narrowing caused by impurity-induced potential fluctuation. However, the related redshift behavior was ultimately not observed through all our measurements compared to the energy gap of an intrinsic material. Even the specimen fabricated with the TEG flow rate high to 3.35 $\mu\text{mol}/\text{min}$ just exhibited a slight decrease in the PL peak energy to 3.393 eV due to the compensation effect of electrons.

IV. CONCLUSIONS

Characterizations of ZnO:Ga films fabricated on p -Si(111) substrates by AP-MOCVD using TEG as the doping gas have been systematically conducted. It was found that the amount of Ga elements doped in ZnO film evidently influence its grain structure, electrical, and optical properties. For the range of TEG flow rate investigated, a flat surface with the predominant orientation of (101) can be obtained for the ZnO:Ga films fabricated at the TEG flow rate over 2.79 $\mu\text{mol}/\text{min}$. Moreover, the TEG flow rates higher than 2.23 $\mu\text{mol}/\text{min}$ can be used to obtain ZnO:Ga films with low

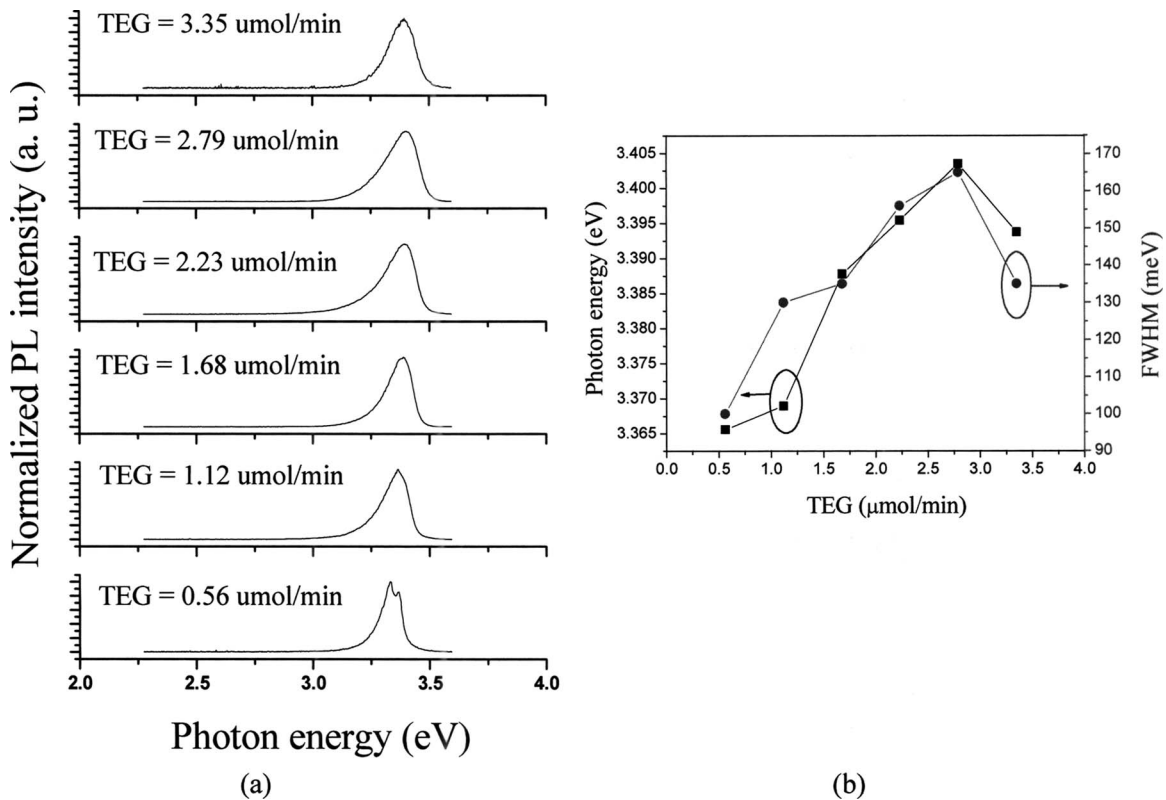


FIG. 5. (a) 12 K PL spectra of ZnO:Ga films fabricated at different TEG flow rates and (b) photon energy and FWHM variations with the TEG flow rate.

resistivity values (10^{-3} – 10^{-4} Ω cm). In particular, the film fabricated at the TEG flow rate = $2.79 \mu\text{mol}/\text{min}$ revealed simultaneously a highest electron concentration of $8.93 \times 10^{20} \text{ cm}^{-3}$, a highest Hall mobility of $15.4 \text{ cm}^2 \text{ V}^{-1} \text{ s}^{-1}$, and also a lowest resistivity of $4.54 \times 10^{-4} \Omega \text{ cm}$. The mobility is considered to be dominated by the grain boundary scattering when the TEG flow rate is lower than $2.79 \mu\text{mol}/\text{min}$, but is dominated by the ionized impurity scattering when the TEG flow rate is higher than $2.79 \mu\text{mol}/\text{min}$. This phenomenon has made a highest mobility be achieved at the TEG flow rate = $2.79 \mu\text{mol}/\text{min}$. In addition, a compensation effect is suggested to explain the decrease in electron concentration after the maximum value is obtained. Combining both the variations of electron concentration and mobility as a function of the TEG flow rate naturally yields a lowest resistivity at the TEG flow rate = $2.79 \mu\text{mol}/\text{min}$. Conclusively, degenerate *n*-type ZnO films can be produced by AP-MOCVD using the Ga-doping technique, which is further characterized by the blueshift (3.365–3.403 eV) and linewidth broadening (100–165 meV) of PL spectra for the specimens fabricated with various TEG flow rates (0.56– $2.79 \mu\text{mol}/\text{min}$).

¹B. Rech and H. Wagner, *Appl. Phys. A: Mater. Sci. Process.* **69**, 155 (1999).

²A. Shimizu, S. Chaisitsak, T. Sugiyama, A. Yamada, and M. Konagai, *Thin Solid Films* **361–362**, 193 (2000).

³J. C. Lee, K. H. Kang, S. K. Kim, K. H. Yoon, I. J. Park, and J. Song, *Sol. Energy Mater. Sol. Cells* **64**, 185 (2000).

⁴D. C. Look, *Mater. Sci. Eng., B* **80**, 383 (2001).

⁵S. J. Pearton, D. P. Norton, K. Ip, Y. W. Heo, and T. Steiner, *Prog. Mater. Sci.* **50**, 293 (2005).

⁶A. F. Kohan, G. Ceder, D. Morgan, and C. G. Van de Walle, *Phys. Rev. B* **61**, 15019 (2000).

⁷K.-K. Kim, S. Niki, J.-Y. Oh, J.-O. Song, T.-Y. Seong, S.-T. Park, S. Fujita, and S.-W. Kim, *J. Appl. Phys.* **97**, 066103 (2005).

⁸T. Makino, Y. Segawa, S. Yoshida, A. Tsukazaki, A. Ohtomo, and M. Kawasaki, *Appl. Phys. Lett.* **85**, 759 (2004).

⁹T. Minami, H. Nanto, and S. Takata, *Jpn. J. Appl. Phys., Part 2* **23**, L280 (1984).

¹⁰K. L. Chopra, S. Major, and D. K. Pandya, *Thin Solid Films* **102**, 1 (1983).

¹¹Y. Li, G. S. Tompa, S. Liang, C. Gorla, Y. Lu, and John Doyle, *J. Vac. Sci. Technol. A* **15**, 1063 (1997).

¹²X. L. Chen, B. H. Xu, J. M. Xue, Y. Zhao, C. C. Wei, J. Sun, Y. Wang, X. D. Zhang, and X. H. Geng, *Thin Solid Films* **515**, 3753 (2007).

¹³X. Yu, J. Ma, F. Ji, Y. Wang, X. Zhang, C. Cheng, and H. Ma, *J. Cryst. Growth* **274**, 474 (2005).

¹⁴X. Yu, J. Ma, F. Ji, Y. Wang, X. Zhang, and H. Ma, *Thin Solid Films* **483**, 296 (2005).

¹⁵Q. B. Ma, Z. Z. Ye, H. P. He, S. H. Hu, J. R. Wang, L. P. Zhu, Y. Z. Zhang, and B. H. Zhao, *J. Cryst. Growth* **304**, 64 (2007).

¹⁶Z. F. Liu, F. K. Shan, Y. X. Li, B. C. Shin, and Y. S. Yu, *J. Cryst. Growth* **259**, 130 (2003).

¹⁷S. J. Henley, M. N. R. Ashfold, and D. Chems, *Surf. Coat. Technol.* **177–178**, 271 (2004).

¹⁸H. Kato, M. Sano, K. Miyamoto, and T. Yao, *J. Cryst. Growth* **237–239**, 538 (2002).

¹⁹J. Hu and R. G. Gordon, *J. Appl. Phys.* **72**, 5381 (1992).

²⁰V. Khranovskyy, U. Grossner, V. Lazorenko, G. Lashkarev, B. G. Svensson, and R. Yakimova, *Superlattices Microstruct.* **39**, 275 (2006).

²¹J. D. Ye *et al.*, *J. Cryst. Growth* **283**, 279 (2005).

²²E. W. Forsythe, Yongli GaO, L. G. Provost, and G. S. Tompa, *J. Vac. Sci. Technol. A* **17**, 1761 (1999).

²³Y. C. Huang *et al.*, *Thin Solid Films* **517**, 5537 (2009).

²⁴B. Hahn, G. Heindel, E. Pschorr-Schoberer, and W. Gebhardt, *Semicond. Sci. Technol.* **13**, 788 (1998).

²⁵N. Nishimoto *et al.*, *J. Cryst. Growth* **310**, 5003 (2008).

- ²⁶O. Nakagawara, Y. Kishimoto, H. Seto, Y. Koshido, Y. Yoshino, and T. Makino, *Appl. Phys. Lett.* **89**, 091904 (2006).
- ²⁷V. Khranovskyy, U. Grossner, V. Lazorenko, G. Lashkarev, B. G. Svensson, and R. Yakimova, *Thin Solid Films* **515**, 472 (2006).
- ²⁸Y. Ma *et al.*, *J. Appl. Phys.* **95**, 6268 (2004).
- ²⁹S. Ghosh, A. Sarkar, S. Chaudhuri, and A. K. Pal, *Thin Solid Films* **205**, 64 (1991).
- ³⁰J. Gutowski, N. Presser, and I. Broser, *Phys. Rev. B* **38**, 9746 (1988).
- ³¹D. C. Reynolds, D. C. Look, and B. Jogai, *Phys. Rev. B* **57**, 12151 (1998).
- ³²B. P. Zhang, N. T. Binh, Y. Segawa, Y. Kashiwaba, and K. Haga, *Appl. Phys. Lett.* **84**, 586 (2004).
- ³³A. Teke, Ü. Özgür, S. Doğan, X. Gu, H. Morkoç, B. Nemeth, J. Nause, and H. O. Everitt, *Phys. Rev. B* **70**, 195207 (2004).
- ³⁴E. Burstein, *Phys. Rev.* **93**, 632 (1954).
- ³⁵T. S. Moss, *Proc. Phys. Soc. London, Sect. B* **67**, 775 (1954).
- ³⁶A. Walsh, J. L. F. D. Silva, and S. H. Wei, *Phys. Rev. B* **78**, 075211 (2008).
- ³⁷J. De-Sheng, Y. Makita, K. Ploog, and H. J. Queisser, *J. Appl. Phys.* **53**, 999 (1982).
- ³⁸S. M. Ryvkin, *Phys. Status Solidi* **11**, 285 (1965).